Self-organization of semiconductor nanocrystals by selective surface faceting

Bin Yang, Pengpeng Zhang, D. E. Savage, and M. G. Lagally*
University of Wisconsin-Madison, Madison, Wisconsin 53706, USA

Guang-Hong Lu, Minghuang Huang, and Feng Liu
University of Utah, Salt Lake City, Utah 84112, USA
(Received 14 October 2005; published 12 December 2005)

The formation and ordering of Si nanocrystals in dewetting and agglomeration of the thin single crystalline Si layer in silicon-on-insulator has been investigated using low-energy electron microscopy. The evolution of the Si dewetting and agglomeration is captured in real time, revealing the detailed process for the formation and ordering of the nanocrystals. A surface faceting mechanism governing this self-organized process is proposed and supported with first-principles calculations.

DOI: 10.1103/PhysRevB.72.235413 PACS number(s): 81.16.Dn, 68.35.Md, 68.37.Nq, 68.65.Hb

Semiconductor nanocrystals have attracted much attention because of their unique properties and potential applications in nanoscale devices.[1–3] A promising method for creating semiconductor nanocrystals on surfaces is free-energy-minimization driven self-assembly. One straightforward approach of this kind, surface self-assembly via the dewetting and agglomeration of thin solid films on a substrate, has been used in a variety of applications, including catalysis,[4,5] storage devices,[6] and sensors.[7]

As the vast majority of thin films deposited on a substrate is thermodynamically unstable, films readily dewet from the substrate and agglomerate into three-dimensional (3D) nanocrystals under appropriate conditions (see review[8]). Agglomerated nanocrystals prepared by dewetting from a substrate are invariably randomly distributed or show fractal characteristics,[8] however, because the films from which they form, prepared by sputter deposition or evaporation on a heterogeneous host, are amorphous or polycrystalline. Random distributions are themselves quite valuable,[5,7] but many bottom-up nanotechnological applications foresee a need for order.[9,10] So far in rare cases, but ones that are rapidly becoming more relevant in semiconductor technology, the thermodynamically unstable thin top layer is crystalline. The outstanding example is silicon-on-insulator (SOI): for this material, the self-organization shows a different behavior. As the thin Si layer dewets from the underlying amorphous-oxide substrate, the agglomerating Si nanocrystals self-order into a very distinctive pattern.[11,12] The physical mechanism underlying such self-organization has not been determinable, because so far only the end pattern has been observed, with very little knowledge of its initiation and progression.

In this paper, we present the first real-time observation of the dewetting and agglomeration process, with a detail that allows insight into the mechanisms of Si nanocrystal formation and organization from an initially continuous thin film as it dewets from the substrate under elevated temperature. We follow the dynamics of the dewetting and self-organized agglomeration with low-energy electron microscopy (LEEM). LEEM shows that the self-organization arises from a selective surface faceting process. First-principles surface energy calculations confirm that the faceting is controlled by surface energy anisotropy. We compare the surface energies of relevant high-temperature Si surface phases, providing a quantitative assessment of the desire of the system to organize in the fashion in which it does. We expect that the concepts we articulate here are general to single-crystal thin films or membranes bonded to or otherwise formed on foreign hosts.

We carry out experiments with bonded SOI. SOI, in which a silicon dioxide layer (200 nm thick here) is interspersed between a crystalline top Si layer (the template layer) and the bottom Si (handle) wafer, is rapidly becoming a mainstream substrate in microelectronics fabrication. Both the template and substrate Si layer are crystalline and (001) oriented. The top Si layer is thinned to the order of 10 nm by dry thermal oxidation and wet chemical oxide etching. The samples are chemically cleaned using the triple IMEC procedure[13] and introduced into the LEEM chamber at a base pressure of 5×10^{-10} Torr and outgassed overnight at 650 °C. The sample is covered by a thin oxide layer, which protects the Si template layer. The sample is rapidly heated to 900 °C for 50 sec in a 5×10^{-8} Torr disilane atmosphere to remove the oxide, and then rapidly cooled.

For thicknesses below the range of tens of nanometers, a clean single-crystal Si template layer dewets at elevated temperatures, leading to self-organized Si nanocrystals that form in squares.[11,12] The edges of the squares are along ⟨110⟩ directions. Inside the squares, Si nanocrystals self-organize into a regular array, exhibiting high spatial and orientational order, in particular lining up along ⟨130⟩ directions.[11,12] Figure 1 shows our results, which are similar to those of Refs. 11 and 12. Important observations are that the Si surface must be clean (the dewetting occurs only if the sample is heated in ultrahigh vacuum) and that the dewetting starts predominantly at defect sites, such as pinholes, indicating a heterogeneous process.

We perform LEEM at UHV ($\sim10^{-10}$ torr) and at various temperatures in the dark-field image mode, using the contrast caused by the electron emission difference between Si and SiO_2,[14] on SOI samples in which the top Si layer has been thinned to the order of 10 nm by dry thermal oxidation and wet chemical oxide etching. Figure 2 shows four sequential LEEM images at five sec intervals, illustrating the dewetting and agglomeration process at 980 °C. The Si template sur-

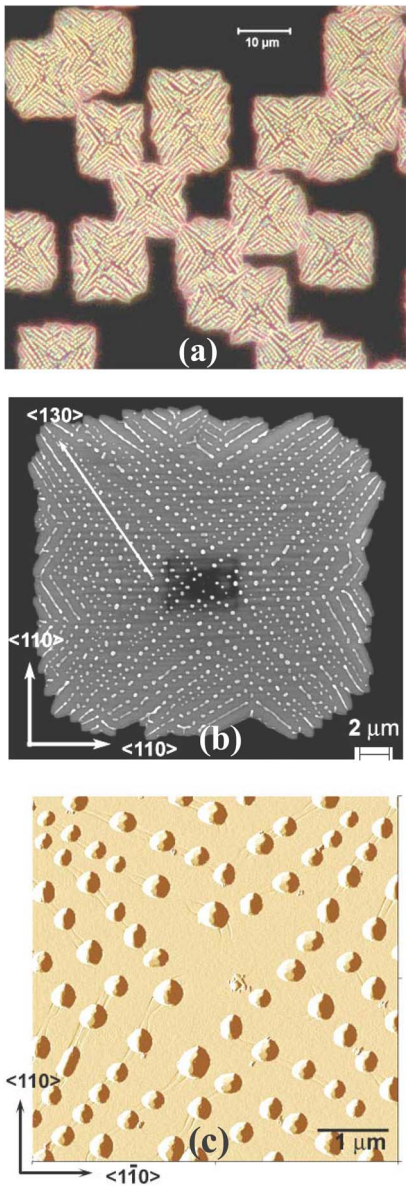

FIG. 1. (Color online) Self-organized Si nanocrystals, formed when a thin (here 9 nm) template layer of Si dewets from the oxide in SOI after annealing at 900 °C for 5 min. The dewetting initiates at defects in the Si layer. (a) Optical image showing a number of regions of dewetting on SOI (1000×). (b) Scanning electron microscopy image showing an ordered array of Si nanocrystals (bright spots) in one agglomeration pattern. (c) Atomic force microscopy image showing the center region of one pattern. The Si nanocrystals are faceted and 90 nm high×300 nm wide on average.

face appears dark and the exposed oxide surface appears bright. The Si layer dewets initially in stripes, beginning at the edges of the remaining complete Si layer, with Si atoms moving away to expose oxide trenches (bright bands) extending out along ⟨130⟩ directions. The already dewetted region is out of the field of view at the bottom (see Fig. 1). Going from Fig. 2(a) and 2(b) one can see a trench extending from position $A1$ to $A2$ along the [130] direction; at the same time, another trench forms and grows from position $B1$ to $B2$ along the [310] direction. This process continues, to form

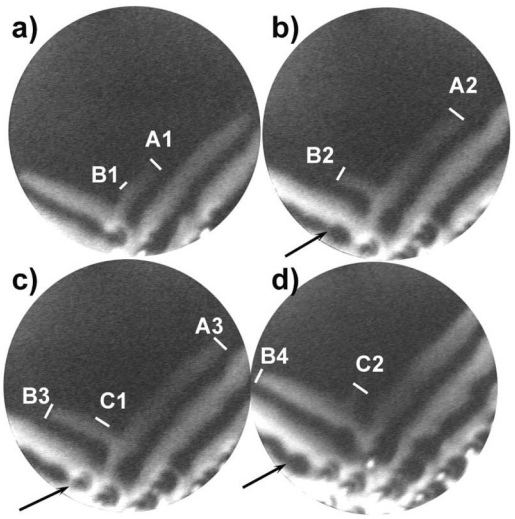

FIG. 2. Real-time sequential LEEM images of the dewetting and agglomeration process in SOI, taken at 5 sec intervals at 980 °C. The image field of view is 5 μm. Labels $A1$ to $A2$, $B1$ to $B2$, and $C1$ to $C2$ indicate formation and growth of trenches in the Si template layer along two ⟨130⟩ directions. The trenches appear as bright bands because the exposed oxide has a higher electron emission. Between trenches, Si ridges (dark bands) form, also along ⟨130⟩ directions. These ridges then narrow, as indicated by arrows in *b*, *c*, and *d*, and break up into individual nanocrystals (dark dots).

eventually a network of trenches all in ⟨130⟩ directions [Figs. 2(c) and 2(d)]. We expect that the width of the trenches is related to the diffusion distance of Si, as very little Si leaves but instead piles up onto the Si ridges between the trenches, which are forced also to be along ⟨130⟩ directions. Finally, the ridges break into individual Si nanocrystals (without loss of volume), as indicated by arrows in Figs. 2(b)–2(d), due to the Rayleigh instability.[15] Naturally, these Si islands line up along ⟨130⟩ directions.

The high-temperature LEEM measurements do not have the ability to resolve the facet structure of the islands. The atomic force microscopy (AFM) measurement of the Si nanocrystals in the fourfold pattern shows that the nanocrystals are facetted, as seen in Fig. 3. The AFM line scans show an angle of 72±2° between the large facets at the island base and the surface, indicating that these are indeed (311) type facets. The islands have [Fig. 3(a)] shallower facets [e.g., (111) and (113)], on their upper parts, as well as continuation surface between the facets.

The temperatures (<980 °C) needed for the dewetting of our Si layers are below the roughening temperature of the Si(001) surface (~1200 °C), and presumably depend on the thickness of the Si layer.[16] We have also confirmed by reflection high-energy electron diffraction (RHEED) measurements that the Si layer has never melted or shown signs of premelting in the above dewetting and agglomeration process.

The real-time LEEM observations, supported by the AFM and RHEED results, lead us to propose the following mechanism of self-organization. The dewetting initiates at pinholes and the concomitant agglomeration at a fixed temperature is controlled by a highly selective surface faceting process,

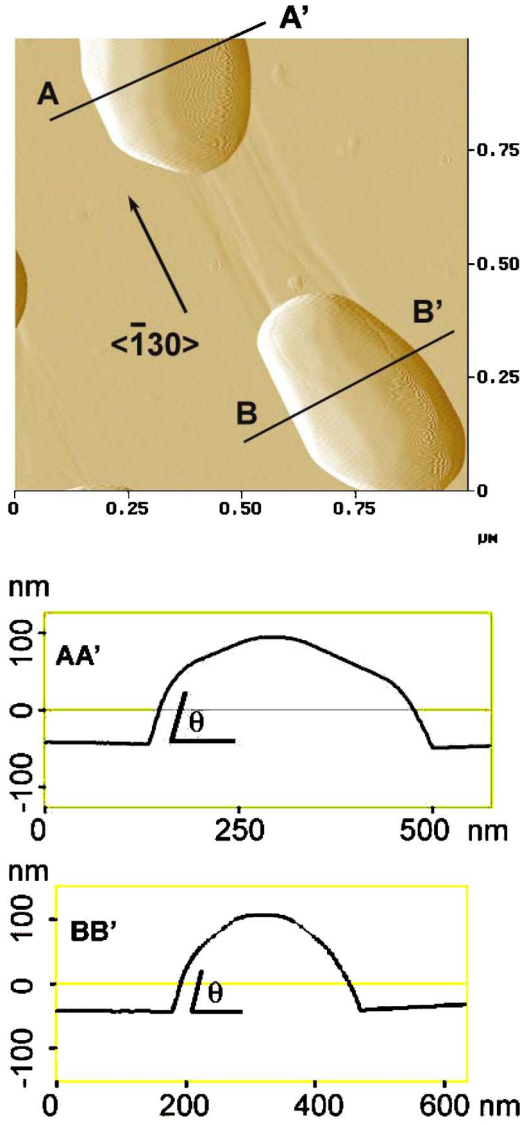

FIG. 3. (Color online) AFM images and line scans of Si nanocrystals. The measured contact angle θ is 72±2° (Ref. 28).

with the surface structures formed during the process, including trenches, ridges, and islands, bounded at their base by a single family of {311} facets, as illustrated in Fig. 4. For example, if a trench is bounded by $(3\bar{1}1)$ and $(\bar{3}11)$ facets, it must grow along the ⟨130⟩ (⟨$\bar{1}\bar{3}0$⟩) direction, i.e., along the intersection line of the $(3\bar{1}1)$ plane (the facet plane) and the (001) plane (surface and interface) calculated as $(3\bar{1}1) \otimes (001) = \langle 130 \rangle$, as shown in Fig. 4. Similarly, if a trench is bounded by (311), (131), or $(1\bar{3}1)$ facets, then it must grow along the ⟨$3\bar{1}0$⟩, ⟨$\bar{3}\bar{1}0$⟩, or ⟨$1\bar{3}0$⟩ directions. Consequently, ridges and hence Si islands will only form along one of these four directions, as shown in Fig. 1. As we discuss below, the trench cannot, however, be bounded by those planes of the {311} family with index, $z=3$, such as a (113) plane, because these planes make a much smaller contact angle with the (001) surface and interface. Otherwise, we would see islands align along the ⟨110⟩ direction, which we do not.

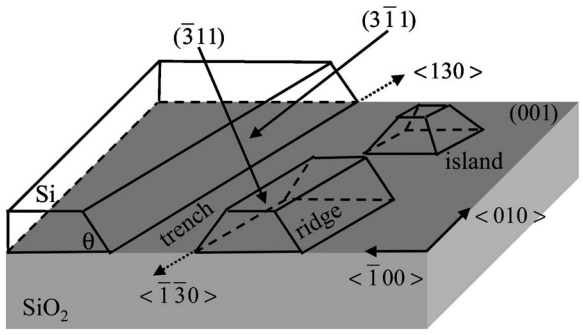

FIG. 4. Schematic diagram illustrating the sequential formation of trenches, ridges, and nanocrystals, all bounded by $(3\bar{1}1)$ and $(\bar{3}11)$ facets, leading to alignment of the nanocrystals in the ⟨130⟩ direction. The contact angle of a $(3\bar{1}1)$ facet with the oxide surface is 72.45°.

The proposed mechanism requires that {131} facets be the most stable ones at the dewetting and agglomeration temperature. We have confirmed this stability by first-principles calculations.[17] We compare the stability of Si {111} and {113} surfaces at high temperature, as both had been considered as the most stable Si facet.[18,19] The structures of both Si(311) and Si(111) surfaces depend on temperature. At high temperature, Si(311) exhibits a (3×1) or (1×1) reconstruction[20,21] and Si(111) a (1×1) reconstruction;[22] at low temperature, Si(311) exhibits a (3×2) reconstruction,[20,23] and Si(111) a (7×7) reconstruction.[22] Our calculations show that at low temperature, the Si(311)-(3×2) phase (95 meV/Å^2) is slightly higher in energy than is the Si(111-(7×7)) phase (89 meV/Å^2); but at high temperature, the Si(311)-(3×1) (96 meV/Å^2) or (1×1) reconstructions (113 meV/Å^2) are more stable than Si(111)-(1×1) (125 meV/Å^2). Thus, at the dewetting temperature, Si(311) facets are preferred over Si(111) facets. Note that we compare only the enthalpies of different surfaces at a relative high temperature (~900 °C), because entropy differences between these surface phases are expected to be small as long as all the surfaces maintain their ordered phases with well-defined reconstruction (atomic ordering). For example, the entropy difference between the 7×7 and 1×1 phases is about $0.013k_B$ per 1×1 cell.[24].

An additional observation favors the proposed mechanism. Although all facets in the ⟨311⟩ family have the same energy, those with index z=3, such as (113) and $(1\bar{1}3)$, do not appear in the agglomerated Si islands as the facets in contact with the oxide surface. This is because the overall formation (nucleation) energy of a facet is not determined by the facet energy alone, but depends also on its orientation with respect to the substrate. Dewetting starts from a pinhole with probably vertical sidewalls. As Si moves, these sidewalls will tilt from the vertical (with an unfavorable energy) to reach a lower-energy configuration, at a faceting angle θ. The formation energy for a given low-energy configuration can be calculated as

$$E_{formation} = \gamma_f \cos\theta + (1/2)(\gamma_i - \gamma_{Si} - \gamma_{SiO_2}), \qquad (1)$$

where f, i, Si, and SiO_2 are, respectively, the surface energies of a facet, the Si/SiO_2 interface, the Si(001) surface, and the SiO_2 surface. For the same facet energy, γ_f, the smaller the angle a facet makes with the surface, the larger is its overall formation energy. The formation energy of a shallow (113) facet, having a (001) surface contact angle of 25.24°, would be three times higher than that of a steep (311) facet, having a contact angle of 72.45°. For the same reason, the (311) facet is energetically favored over the (111) facet even if they had comparable surface energies, because the (111) facet is shallower, with a smaller contact angle of 54.75°. The surface contact angle is uniquely defined for and by the given facet, unlike the equilibrium contact angle of a liquid droplet, which is not limited to discrete values but takes the value that minimizes the free energy.[25] Consequently, for two facets with degenerate energies, the facet with a steeper surface contact angle will form because of a smaller surface area.

Furthermore, possible kinetic limitations also favor the steep (311) facet, the first with a low energy that the system can reach. As the silicon atoms moving away from the vertical wall of the initial sites, the system will reach the steep (311) facets first. Even if the formation energies were similar, there would be no motivation for the system to go beyond the (311) facet.

In conclusion, we have used real-time LEEM imaging combined with AFM, RHEED, and first-principles calculations to identify and quantify the mechanism of formation and self-organization of Si nanocrystals when the thin single-crystal Si template layer in SOI dewets. The self-organization is driven by a surface energy anisotropy, which leads to predominant formation of surface structures controlled by a single low-energy facet. Thermally unstable single-crystal thin films or membranes on isotropic or amorphous substrates or other foreign hosts, for example, wafer bonded or transferred multilayer structures with thin top layers, such as Ge-on-insulator, GaN on sapphire, GaAs on SOI, etc., or dopant or implant-isolated thin layers, are currently rapidly gaining favor as a form of nanomaterial. We would expect that such systems would similarly show unique agglomeration patterns that reflect the thermodynamically stable facets. Patterns of agglomerated nanocrystals, far from being just a nuisance or an item of only scientific interest, may themselves serve as templates for formation of organized nanostructures or as arrays that can serve useful purposes in nanoelectronic and nanophotonic applications.[26,27]

We thank P. P. Rugheimer, M. M. Roberts, and F. Flack for helpful discussions. This research was supported by DOE Grant No. DE-FG03-03ER46027 and Grant No. DE-FG02-03ER46028.

*Electronic address: lagally@engr.wisc.edu

[1] S. Fafard, Z. R. Wasilewski, C. N. Allen, K. Hinzer, J. P. McCaffrey, and Y. Feng, Appl. Phys. Lett. **75**, 986 (1999).
[2] V. M. Ustinov, E. R. Weber, S. Ruvimov, Z. Liliental-Weber, A. E. Zhukov, A. Y. Egorov, A. R. Kovsh, A. F. Tsatsulikov, and P. S. Kop'ev, Appl. Phys. Lett. **72**, 362 (1998).
[3] T. Lundstrom, W. Schoenfeld, H. Lee, and P. M. Petroff, Science **286**, 2312 (1999).
[4] R. S. Wagner and W. C. Ellis, Appl. Phys. Lett. **4**, 89 (1964).
[5] M. Yudasaka, R. Kikuchi, T. Matsui, Y. Ohki, S. Yoshimura, and E. Ota, Appl. Phys. Lett. **67**, 2477 (1995).
[6] S. Tiwari, F. Rana, H. Hanafi, A. Hartstein, E. F. Crabbe, and K. Chan, Appl. Phys. Lett. **68**, 1377 (1996).
[7] S. K. Sharma and J. Spitz, Thin Solid Films **66**, L51 (1980).
[8] D. J. Srolovitz and M. G. Goldiner, JOM **47**, 31 (1995).
[9] C. S. Lent and P. D. Tougaw, Proc. IEEE **85**, 541 (1997).
[10] C. T. Black, C. B. Murray, R. L. Sandstrom, and S. H. Sun, Science **290**, 1131 (2000).
[11] R. Nuryadi, Y. Ishikawa, and M. Tabe, Appl. Surf. Sci. **159**, 121 (2000).
[12] R. Nuryadi, Y. Ishikawa, Y. Ono, and M. Tabe, J. Vac. Sci. Technol. B **20**, 167 (2002).
[13] A. W. Woll, P. Moran, E. M. Rehder, B. Yang, T. F. Kuech, and M. G. Lagally, Mater. Res. Soc. Symp. Proc. **696**, 119 (2002).
[14] S. Yamamoto, S. Masuda, H. Yasufuku, N. Ueno, Y. Harada, T. Ichinokawa, M. Kato, and Y. Sakai, J. Appl. Phys. **82**, 2954 (1997).
[15] L. Rayleigh, Proc. London Math. Soc. **10**, 4 (1878).
[16] J. B. Maxson, D. E. Savage, F. Liu, R. M. Tromp, M. C. Reuter, and M. G. Lagally, Phys. Rev. Lett. **85**, 2152 (2000).
[17] G. H. Lu, M. H. Huang, M. Cuma, and F. Liu, Surf. Sci. **588**, 61 (2005).
[18] D. J. Eaglesham, A. E. White, L. C. Feldman, N. Moriya, and D. C. Jacobson, Phys. Rev. Lett. **70**, 1643 (1993).
[19] J. M. Bermond, J. J. Metois, X. Egea, and F. Floret, Surf. Sci. **330**, 48 (1995).
[20] U. Myler and K. Jacobi, Surf. Sci. **220**, 353 (1989).
[21] J. Schreiner, K. Jacobi, and W. Selke, Phys. Rev. B **49**, 2706 (1994).
[22] K. Takayanagi, Y. Tanishiro, S. Takahashi, and M. Takahashi, Surf. Sci. **164**, 367 (1985).
[23] J. Knall, J. B. Pethica, J. D. Todd, and J. H. Wilson, Phys. Rev. Lett. **66**, 1733 (1991).
[24] J. B. Hannon, J. Tersoff, and R. M. Tromp, Science **295**, 299 (2002).
[25] F. Liu, Phys. Rev. Lett. **89**, 246105 (2002).
[26] B. Yang, M. S. Marcus, D. G. Keppel, P. P. Zhang, Z. W. Li, B. J. Larson, D. E. Savage, J. M. Simmons, O. M. Castellini, M. A. Eriksson, and M. G. Lagally, Appl. Phys. Lett. **86**, 263107 (2005).
[27] H. C. Yuan, B. Yang, J. M. Simmons, M. S. Marcus, Z. Q. Ma, M. A. Eriksson, and M. G. Lagally, Proc. SPIE **5971**, 289 (2005).
[28] The measurement is done with a tip with a 15° front angle and 25° back angle. The typical mounting angle is about 10°. Because of the tip geometry, measurements on the front slopes shallower than 75° are reliable, but not on backside slopes steeper than 65°. Consequently, the angles at the front edges (left sides of the islands) are accurate, but the angles at the back edges (right sides) are not.